

Rock Mechanics and Rock Engineering

A reliability-based approach for the design of rockfall protection fences

--Manuscript Draft--

Manuscript Number:	
Full Title:	A reliability-based approach for the design of rockfall protection fences
Article Type:	Original Paper
Keywords:	rockfall protection structures; discrete element model; reliability analysis
Corresponding Author:	Franck Bourrier, Ph.D. Irstea - UR EMGR Saint Martin d Heres, FRANCE
Corresponding Author Secondary Information:	
Corresponding Author's Institution:	Irstea - UR EMGR
Corresponding Author's Secondary Institution:	
First Author:	Franck Bourrier, Ph.D.
First Author Secondary Information:	
Order of Authors:	Franck Bourrier, Ph.D.
	Stéphane Lambert, Ph. D.
	Julien Baroth, Ph. D.
Order of Authors Secondary Information:	
Abstract:	<p>This paper proposes a method for improving the design of rockfall protection fences, accounting for the variability of the loading cases. It is based on a probabilistic reliability analysis and allows combining loading cases issued from rockfall propagation simulations together with numerical simulations of the structure response to the block impact. The interest in such a reliability-based approach is to obtain statistically relevant results concerning the efficiency of the fence in stopping the block with a limited number of simulations. The method was employed on a real study case, involving a low-energy tree-supported fence placed on a forested slope. The trajectory simulations were conducted using RockyFor3D and the fence was modeled using a three-dimensional discrete element method -DEM- model. In a demonstration purpose, two parameters were considered : the block velocity and its angle of incidence before impact. The probability for the fence to be cleared by the block was evaluated accounting for the variability of these two parameters separately or together, either considering these variables non correlated or correlated. The interest of such an approach is demonstrated in terms of computation cost. Besides, the results revealed the importance in accounting for both these parameters for designing the structure as well as for estimating the residual hazard, down the protective structure.</p>

A reliability-based approach for the design of rockfall protection fences

F. Bourrier · S. Lambert · J. Baroth

Received: date / Accepted: date

Abstract This paper proposes a method for improving the design of rockfall protection fences, accounting for the variability of the loading cases. It is based on a probabilistic reliability analysis and allows combining loading cases issued from rockfall propagation simulations together with numerical simulations of the structure response to the block impact. The interest in such a reliability-based approach is to obtain statistically relevant results concerning the efficiency of the fence in stopping the block with a limited number of simulations. The method was employed on a real study case, involving a low-energy tree-supported fence placed on a forested slope. The trajectory simulations were conducted using RockyFor3D and the fence was modeled using a three-dimensional discrete element method -DEM- model. In a demonstration purpose, two parameters were considered : the block velocity and its angle of incidence before impact. The probability for the fence to be cleared by the block was evaluated accounting for the variability of these two parameters separately or together, either considering these variables non correlated or correlated. The interest of such an approach is demonstrated in terms of computation cost. Besides, the results revealed the importance in accounting

F. Bourrier
Irstea, UR EMGR, F-38402 St-Martin-d’Hères, France
E-mail: franck.bourrier@irstea.fr

S. Lambert
Irstea, UR ETGR, F-38402 St-Martin-d’Hères, France
E-mail: stephane.lambert@irstea.fr

J. Baroth
Joseph Fourier University, Grenoble INP, UMR5521 3SRLab, DU, 38041 Grenoble cedex 9, France
E-mail: julien.baroth@ujf-grenoble.fr

for both these parameters for designing the structure as well as for estimating the residual hazard, down the protective structure.

Keywords rockfall protection structures · discrete element model · reliability analysis

1 Introduction

Protection against rockfall hazard often requires building passive protection structures, such as embankments or fences, forming obstacles on the block's route down the slope. The choice between these two countermeasures types is governed by the block kinetic energy and topographic constraints mainly. Fences are widely used to protect roads, railways and buildings downhill steep slopes, from rock blocks with energies up to 5,000 kJ and sometimes more.

Fences consist of an interception structure, a support structure and connecting components, most often made of metallic elements such as a net, posts and cables [11]. For energies less than 100 kJ , support structures generally consist of fixed posts. For higher energies, cables anchored in the soil and connected to the top of the posts are necessary. Moreover, above a 500-kJ energy, friction brakes are used to reduce the force transmitted to these cables and their anchorage, with the aim of dissipating the energy while resulting in large displacements of the fence.

Similarly as for embankments, the design of fences successively addresses their ability in intercepting the block trajectory and their ability in withstanding the impact, respectively referred to as functional and structural designs [18]. Both these design facets require data issued from rockfall propagation simulations. The trajectory simulation tools used for this purpose provide the design engineer with the statistical distributions of the passing height and velocity of a given block of a certain mass at any given point on the slope [5].

Classically, the functional design, which aims at defining the fence interception height, considers the block passing height distribution while the structural design mainly consider the block kinetic energy distribution. For both these parameters, a statistical estimator of the distribution is considered (95% quantile, for example), so that only a very limited percentage of blocks are not caught by the structure or destroy it.

For the last two decades, rockfall protection fences have received substantial attention through experimental and numerical investigations [20,19,12,16,14,25,4,24,23]. Reviews of these studies can be found in [14] and [20]. The vast majority of the studies conducted to date concerns fences intended to intercept blocks with kinetic energies from 1 to more than 5 MJ as the demand for protection against catastrophic events is very high. The real-scale tests conducted in the frame of the technical agreement process covering fences in Europe (EOTA, 2008) contributes to the research on the actual response of these flexible barriers and provides validation data for the numerical models developed in parallel [4,13].

Despite the recent advances concerning the impact response of fences, limitations concerning their design can be identified. First, experimental results on which are based recent developments mainly concern centered impacts, by a block with a normal to the fence pre-impact trajectory and without rotational velocity. Second, rockfall fences designed for energies amounting to 200 *kJ* or less have been marginally studied while they concern a large number of sites [15,8,7]. Third, the fence design rarely considers the block impact location on the fence, the block rotational kinetic energy nor the trajectory inclination with respect to the fence. And finally, the variability associated to the different design parameters is not accounted for.

Nonetheless, the numerous numerical tools that have been developed for modelling the impact response of fences could be envisaged to address the points cited above. Such models can be used to assess the efficiency of existing structures types and develop new ones or to analyze the response for loading cases representative for the distribution of the block trajectories before impact. But on a practical point of view, such studies would require conducting large number of simulations to obtain statistically relevant results, resulting in nonaffordable computation times.

This paper proposes an alternative methodology based on reliability analyses [1] to overcome this key limitation to the use of numerical models for the design of rockfall protection fences. In the methodology proposed, a probabilistic modeling of the loading is deduced from the rockfall simulations. The probability of clearing of the fence under the probabilistic loading from the rockfall simulation is calculated from a reduced number of impact simulations using a specific probabilistic method [2]. The fence design methodology is applied to a real case study focusing on two parameters of importance in the design of fences, namely the block impact velocity and the impact angle.

2 Study case

2.1 A tree-supported structure for low energy impacts

This paper deals with a peculiar type of structure using trees in place of man-made supporting posts (Fig. 1). The fence is made of double-twisted wire mesh, a widespread and easily available product. It is connected to an upper and a lower cables thanks to cable clips regularly spaced. Each cable extremity forms a loop around a tree-trunk, the cable dead end being secured on the cable by cable clips. The loops are loosely tightened to avoid any damage to the trunk. Two rigid posts placed at each extremity of the fence, parallel to the tree trunks, maintain the distance between the upper and lower supporting cables.

This type of structure is particularly adapted for forested slopes where wood felling practice or forest road opening can initiate rockfall. Its installation does not require heavy machinery for soil moving or nailing, preserving the forest stand. Besides, it is rapid and easy to install and remove, making these

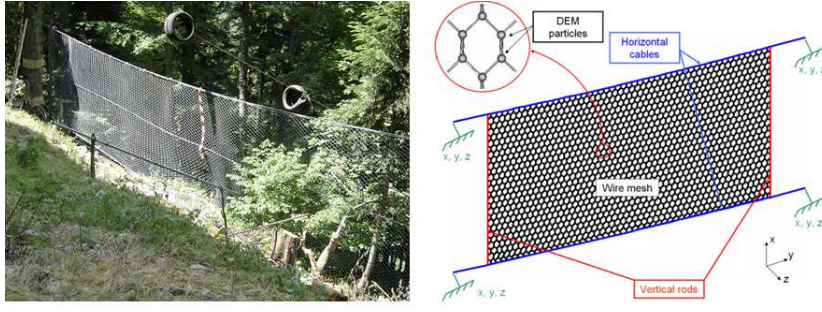


Fig. 1 Tree-supported fence : experimental structure and DEM model

tree-supported structures also an adequate solution for temporary protection purpose, as for instance during works on the slope.

Using trees as supports instead of posts globally simplifies the installation. However, the design of the structure must account for the mechanical characteristics of the tree, that depends on the tree diameter and species [10] and on the anchorage of the root system [22]. Besides, the selected trees must be at the same altitude to build a fence perpendicular to the average trajectory of the falling blocks, and at an appropriate distance one to the other.

In such a context, rock blocks involved can vary in weight from 1 *kg* to less than 1 *ton*, with velocities less than 25 *m/s*, the maximum velocity of blocks on forested slopes reported in the literature [10]. Therefore, kinetic energies less than 200 *kJ* can be expected, which is considered a low-energy value for rockfall protection structures.

Several on-site impact test campaigns were conducted on these structures validating the concept and providing data for the numerical model calibration [6,17]. The distance between the trees was 22 *m*. The upper and lower supporting cables were 12 *mm* in diameter. The mesh was made of a 2.7-*mm*-diameter wire forming hexagons 80 *mm* and 100 *mm* in height and width respectively. The distance between the support cables, or fence height, was 3 *m*. The distance between the trees and the post was 3 *m*. These parameters were considered in the numerical model presented hereafter.

2.2 Numerical model of the fence

The structure response was simulated based on the discrete element method (DEM) [9] using the open-source software Yade-DEM [21]. DEM models consider the structure as a set of particles interacting one with each other. The interaction force between a pair of particles is computed at each time step from the interparticular distance resulting from the previous time step calculations and considering the mechanical characteristics of the structure between the particles. Then, the resultant of the forces acting on each particle is computed before deriving its displacement using Newton's second law.

The tree-supported fence was modeled accounting for the geometry of the fence, the cables and rods, and the boundary conditions (Fig. 1). The supporting trees were modelled as fixed points assuming the trees to be much more rigid than the structure. Particles associated to the mesh were located at the intersections of wires while particles associated to linear elements (i.e. cables and posts) were distributed along these elements. The mass given to each particle depended on the type of element it was associated to.

In this structure, four different interparticular link types can be distinguished : single wire and double-twist wire of the wire mesh, post and supporting cable. The forces associated to single and double-twist wires were computed using a specific interaction model available in Yade-DEM. The algorithm is based on the model proposed by [3]. It has been recently implemented in the software and proved efficient in modeling the response of an hexagonal wire mesh in different conditions [23]. The single wire stress-strain response considered in the model is identical to that given in [3]. As proposed by these authors, the stress-strain response curve of the double-twist wire is derived from that of the single wire one using the parameters λ_k and λ_e . In this study, these parameters were given the value of 0.62 and 0.1, respectively.

Forces between particles located along the upper and lower cables were calculated considering an elastic model fully characterized by the cable diameter and its Young modulus (140 *GPa*). As sliding of the cable clips was observed during the experiments for a cable tension of about 40 *kN*, an elastoplastic model was considered for particles representing the cable between the tree and the post. The elastic model is considered up to a force of $F_{slip} = 40 \text{ kN}$. Once this threshold value is reached, the inter particular distance is increased so that the interaction force equals F_{slip} . The two vertical posts at the extremities of the wire mesh were modeled as perfectly rigid assemblies of particles.

The impact by the rock block was modeled by considering a spherical element with a given mass and initial velocity. The interaction between the block and the mesh particles was modeled by contact forces considering an elastic normal contact law, with a block Young modulus of 100 *GPa*, and neglecting the block-fence friction. The resultant force on each particle of the mesh is therefore the sum of the contact force with the projectile and of the interaction forces with the adjoining mesh particles. The force applied to the projectile is the sum of all contact forces with the wire mesh particles.

In a first phase, a simulation under gravity loading is held to reach the static equilibrium of the structure. Second, the impact is simulated. The spherical projectile is located at the impact point and initial kinematic conditions are applied to the projectile. For each impact simulation, the time evolutions of the forces in the cables and on the projectile were recorded as well as the projectile trajectory.

The numerical model was used to investigate the influence of parameters related to the block (mass, velocity, impact point, inclination). The influence of various structural choices might also be investigated in an optimization process (single mesh dimensions, fence length, cable diameter).

2.3 Study site

The choice was made to use an extensively documented field rockfall experimental site. The study area covers an Alpine slope ranging from 1200 *m* to 1400 *m* above sea level with a mean gradient of 38° in the 'Forêt Communale de Vaujany' in France (lat. $45^\circ 12'$, long. $6^\circ 3'$). The slope surface mainly consists of rockfall deposits.

For the analysis, the 3D rockfall simulation code Rockyfor3D was used. This software allows simulating the propagation of spherical falling blocks by successive phases of free flight and rebound on the slope surface on a digital terrain model from user-defined departure zones. For the purpose of this study, a digital terrain model with a 2 *m* resolution was used. Additionally, the slope surface material parameters calibrated in the previous research works on the study site have been used [10, 5].

On the contrary, departure zones and falling block volumes different from the previous research works have been defined. The block mass and the location of the departure zone were imposed to obtain rockfall events that can potentially be stopped with low energy rockfall fences. This corresponds to impacting block energy smaller than 50 *kJ*. The purpose of the study case being to protect the forest road located at mid slope of the site from the defined events, the case of a 0.2 *m*³ block weighing 476 *kg* that is reactivated uphill the forest road was envisaged (Fig. 2). The initial falling height of the block was set at 0.5 *m* which corresponds to the lower falling height entailing propagation of the blocks from the release point to the forest road. In this simulation, the projected fence was located at an intermediate distance between the block release point and the forest road to be protected (Fig. 2).

The results from the rockfall simulations are intended to characterize the loading conditions of the fence.

In the numerical model, the fence is assumed to be located at the limit between raster cells. Consequently, for each block release, the kinematics of the block was recorded at the time when the block crosses the fence. All the quantities defining the block kinematics have been measured along the block propagation plane. Along this plane, the block kinematics when reaching the fence is fully characterized by the norm V_r of its translational velocity, the norm ω_r of its rotational velocity, and the impact angle α_r (Fig. 3).

Due to the resolution of the digital terrain model (2 *m*) and the type of digital terrain model (raster map), the horizontal and vertical location of the impact point for the different block release simulations cannot be extracted precisely from the simulations. Both the horizontal and vertical location of the impact point are strongly related with micro topographical changes that are not included in the digital terrain model due to its resolution. Given the potential errors on the estimation of the location of the impact point, it was assumed to be located in the centre of the fence.

Fig. 4 presents distributions of trajectographic characteristics, resulting from rockfall simulations. These figures show a significant variability of the kinematical parameters of the blocks when approaching the fence.

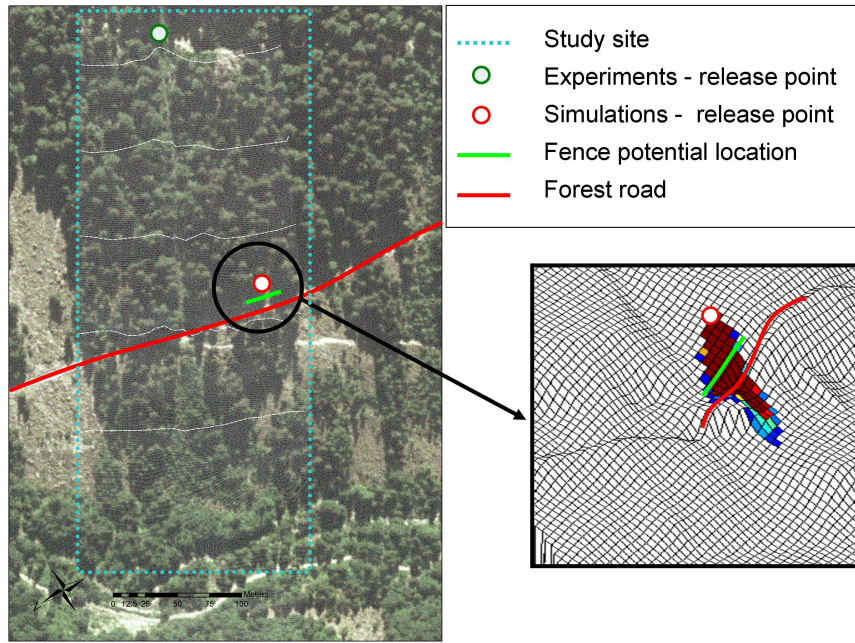


Fig. 2 Definition of the block release point and fence location in the simulations.

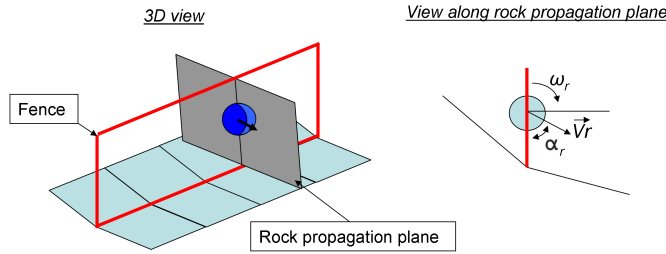


Fig. 3 Parameters describing the block trajectory when crossing the fence.

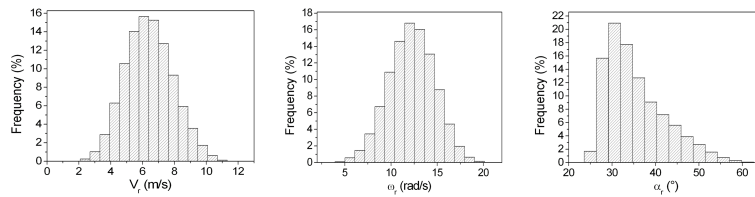


Fig. 4 Block kinematics when reaching the fence obtained from rockfall simulations: distributions of the translational velocity V_r , rotational velocity ω_r , and impact angle α_r .

The design of the net based on a reliability approach should allow defining the fence failure probability (i.e. resulting from its clearing) accounting for the variability of the kinematical parameters of the block V_r , α_r , and Ω_r and of the impact point location characterized by the vertical and horizontal location of the block.

However, performing such an approach is very tricky in practice given the large amount of random variables mentioned above and the potentially significant correlations between these variables. As the first objective of the study was to evaluate the interest of using reliability-based approaches for the design of rockfall fences, the number of random variables considered was limited to the parameters that were expected to have the higher influence on the fence efficiency.

3 Reliability-based design of the fence

The design of the fence first address its efficiency in intercepting the block trajectory : this functional design aims at defining the height of the structure, mainly based on the block passing height issued from trajectory simulations. Then, the structural design is conducted, with the aim of assessing the efficiency of the structure to stop the block once its trajectory intercepted. The approach proposed for this purpose consists in estimating the probability for the block to trespass (or clear) the fence given the distribution of the block kinematics and properties (mass, in particular). For that purpose a criterion for defining the fence clearing by the block is first defined. Second, reliability analyses are held to calculate the probability for this limit criterion to be reached.

3.1 Response modes and efficiency criterion

Experiments and simulations conducted on this type of structure [6,17] revealed that in case of block trajectory interception, five different responses in terms of post-impact block trajectory may be observed :

- the block passes through the fence (mode A),
- the block is rejected uphill by the fence (mode B),
- the block is trapped in the fence, the wire mesh fringed by the lower cable forming a pocket containing the block (mode C),
- in an initial downward displacement the block rotates while in contact with the fence for finally passing below the lower cable (mode D),
- in an initial upward displacement the block rotates while in contact with the fence for finally passing above the upper cable (mode E).

Basically, modes A, D and E result in the clearing of the fence, while modes B and C result in a stopped block. Only mode A necessarily involves damage to the structure. The occurrence of one of these modes depends on the

block translational and rotational incident velocities, incident angle and impact point on the structure. Some modes are rare compared to others and suppose a very peculiar block kinematics (modes D and E). Mode E, that requires an impact closed to the upper supporting cable by a block with an upward trajectory and high rotational velocity, has been observed a few times based on simulations but not during experiments. On the contrary, mode D requiring an impact closed to the lower cable by a block with a downward trajectory has been observed in both the simulations and experiments. However, the block velocity after passing the fence is small resulting in a block generally stopped just after passing the fence. Additionnally, this situation can easily be avoided in practice, adding a wire mesh panel placed on the slope uphill the fence and connected to its lower cable. The case where the fence is punctured (mode A) is the most critical as the post-impact block trajectory is valley-side oriented with a possible high velocity.

The evolution of the block velocity during its interaction with the net fence can be considered for evaluating the fence efficiency. More precisely, the evolution of the sign of the horizontal component of the velocity during impact is a simple and straightforward way for assessing the response of the fence in all the cases exposed above. Indeed, if the block is trapped or pushed uphill by the fence, the horizontal velocity of the block is initially positive and decreases during impact to reach a nil or negative value after impact. On the contrary, if the block passes through, above or below the fence during impact, the horizontal velocity of the block decreases but does not reach negative or nil values.

This analysis naturally leads to consider $G = V_{z,out}/V_{z,in}$ as an estimator of the efficiency of the structure, where $V_{z,in}$ and $V_{z,out}$ are the components along the horizontal z-axis of the block velocity before and after contact with the fence, respectively. $G \leq 0$ means that the block is stopped (safety domain, modes B and C). On the contrary, the block has cleared the fence if $G > 0$, either according to modes A, D or E (failure domain).

3.2 Principles of the reliability-based approach

This section presents the methodology to characterize the probability $P_f = Prob(G > 0)$ for the fence failure using the DEM model of the fence. Contrary to classical Monte Carlo simulations, the approach proposed does not require covering all the parameter ranges. On the contrary, it allows calculating P_f using only a very reduced number of impact simulations, which ensures its practical feasibility. Besides, the loading parameters to be used in the simulations (incident angle, block velocity...) do not result from a user choice : the method allows determining these values to get statistically relevant responses of the structure.

The variability of the impact conditions can be characterized by a set of uncertain parameters y_i associated with the properties of the block (mass,

shape) and its trajectory (impact velocities, impact point location). These parameters can be considered as the different components of a vectorial random variable \mathbf{Y} with a probability density function $p_{\mathbf{Y}}$.

In this context, the mechanical response of the fence is modeled by a random variable $\mathbf{Z} = f(\mathbf{Y})$ to be characterized. In this study, this response is the estimator of the fence efficiency $G = V_{z,out}/V_{z,in}$, called "performance function". Assuming that \mathbf{Y} can be related with a standard random variable \mathbf{X} (Gaussian), such as $\mathbf{Y} = T(\mathbf{X})$, the performance function is expressed as $G = f \circ T(\mathbf{X})$. The appendix provides an example of Gaussian standardization of two correlated log-normal random variables.

In case of one uncertain input parameter $(Y_1) = \mathbf{Y}$, the performance function G may be approximated in writing the approximation \tilde{G} of G as an expansion in Lagrange polynomials [2] of standard Gaussian random variables X , such that

$$G(\mathbf{X}) \simeq \tilde{G}(X) = \sum_{i=1}^N G_i L_i(X) \quad (1)$$

where $G_i = G(x_i)$ is a set of N values of G and L_i are Lagrangian polynomials. For instance, $L_i(X)$ writes

$$L_i(X) = \prod_{\substack{k=1 \\ k \neq i}}^N \frac{X - x_k}{x_i - x_k} \quad (2)$$

Similarly, in case of two uncertain input parameters $(Y_1, Y_2) = \mathbf{Y}$, the performance function G may be approximated, such that

$$G(\mathbf{X}) \simeq \tilde{G}(X_1, X_2) = \sum_{i=1}^N \sum_{j=1}^N G_{i,j} L_i(X_1) L_j(X_2) \quad (3)$$

where $G_{i,j} = G(x_i, x_j)$ is a set of N^2 values of G and L_i, L_j are Lagrangian polynomials.

The calculation of the performance function can be envisaged for a larger number of uncertain input parameters although it will not be presented in the following. The values x_i and x_j are related to collocation points $y_i = T(x_i)$ and $y_j = T(x_j)$. The values y_i and y_j are defined depending on the statistical law associated with the random variable \mathbf{Y} and on the number N of points considered [2].

The values of the performance function $G(x_i)$ (resp. $G(x_i, x_j)$) are thus obtained from numerical simulations of impact on the fence using the set of parameters y_i (resp. (y_i, y_j)) corresponding to x_i (resp. (x_i, x_j)). Then, the numerical (and time-consuming) performance function G is approximated by the analytical function \tilde{G} .

Table 1 Loading conditions used for the design of the fence.

Rock mass	Impact point	α_r	Ω_r	V_r
476 kg	Centred	Random variable	12.24 rad/s	Random variable

Table 2 Means and coefficients of variation of the log-normal random variables associated with the velocity V_r and impact angle α_r , with correlation coefficient $\rho_{Y_1 Y_2} = -0.48$.

Uncertain parameter	$Y_1 = V_r$	$Y_2 = \alpha_r$
Means	$\mu_{Y_1} = 6.42 \text{ m/s}$	$\mu_{Y_2} = 35.39^\circ$
Coefficients of variation	$Cv_{Y_1} = 0.25$	$Cv_{Y_2} = 0.18$

A large number of Monte Carlo simulations are then applied to \tilde{G} to obtain an approximation $\tilde{p}_G = p_{\tilde{G}}$ of the probability density function p_G of G . From this statistical distribution, the cumulative distribution function P_G and the probability $P(G > 0)$ can be evaluated.

3.3 Application to the study case

In the frame of this study and for demonstration purpose, two variables are used for the impact simulations : the impact velocity V_r and the impact angle α_r . The rotational velocity Ω_r was set at the mean value obtained from rockfall simulations considering that this parameter was of second order influence in the simulation results. Basically, this is justified by the low friction angle between the block and the fence, resulting in a negligible influence on the block post-impact trajectory and on the fence mechanical response. The loading conditions used in the following design phase are summarized in Table 1.

As shown in Figure 5, the probability density functions resulting from the trajectory analysis for these two parameters can be satisfactorily modelled using log-normal laws. The log-normal law choice is a satisfying compromise taking into account the trend of histograms and preventing from negative realizations (negative impact velocities, in particular) while allowing an easy probabilistic treatment.

Besides, the different values of the couples (V_r, α_r) show significant negative correlation between the two random variables (Fig. 6). For increasing values of V_r , decreasing mean values and variability of α_r are observed. This correlation can either be ignored or accounting for in evaluating the fence efficiency. In this latter case, a linear correlation can be considered, with a coefficient of -0.48.

Table 2 presents means and coefficients of variation and coefficient of correlation of the random variable.

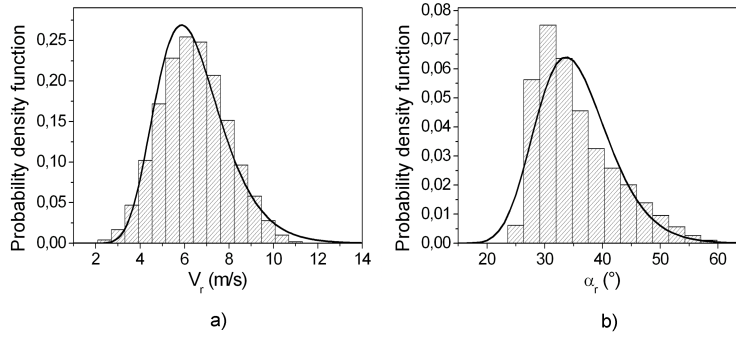


Fig. 5 Approximation of the simulated distribution of V_r and α_r by log-normal laws.

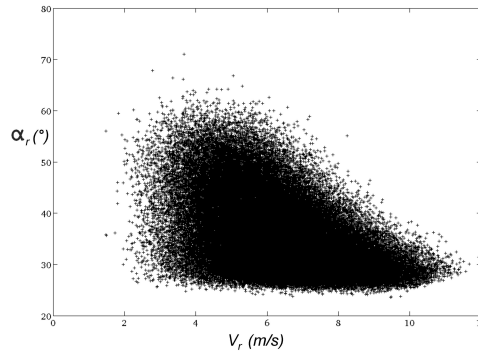


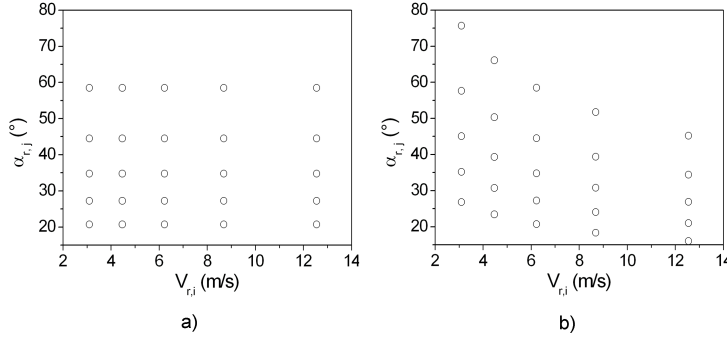
Fig. 6 Couples (V_r, α_r) obtained from rockfall simulations.

In the following, the influence of these two parameters on the efficiency of the fence will be studied first separately and then conjointly. In this latter case, these two parameters are first considered as non correlated before accounting for the linear correlation. In this aim, the two variables (namely the impact velocity V_r and the impact angle α_r) are modelled as two correlated log-normal random variables, denoted $(Y_1, Y_2) = \mathbf{Y}$. As detailed in the appendix, the Gaussian standardization of \mathbf{Y} , using the relation $\mathbf{Y} = T(\mathbf{X})$, is used to apply the collocation method. One or two non correlated variables can be considered using this framework by using only the expression of Y_1 or setting the correlation coefficient $\rho_{Y_1 Y_2}$ at nil value, respectively.

A 5 points procedure ($N = 5$, section 3.2) has been used for analysing the fence failure probability. This means that considering only one random variable, 5 impact simulations are required to estimate the failure probability. If two random variables are considered, a 5 points procedure requires performing impact simulations for all possible couples of the random variables using 5 different values of both random variables, corresponding to 25 impact simulations.

Table 3 Values of the impact velocity $V_{r,i}$ and the impact angle $\alpha_{r,j}$ used in the simulations.

$V_{r,i}$ (m/s)	3.10	4.47	6.23	8.69	12.55
$\alpha_{r,j}$ ($^{\circ}$)	20.72	27.22	34.81	44.53	58.49

**Fig. 7** Couples (V_r, α_r) used for the generation of the simulation sets composed of 25 impact simulations considering non correlated (a) or correlated (b) random variables. Each circle corresponds to a specific couple (V_r, α_r) used for one impact simulation.

A first set of 25 impact simulations was generated for analyzing the fence clearing. The loading cases were defined according to the principle defined in Table 1 and considering the values presented in Table 3 for the impact velocity and the impact angle. The results were analyzed considering first the impact velocity V_r as a random variable. The fence failure was analyzed under this assumption for the different values of the impact angle α_r .

Second, the complete set of simulations was used for analyzing the fence clearing considering both parameters as non correlated random variables.

Finally a second set of 25 impact simulations was generated to analyse the fence clearing considering the correlation between the two random variables.

The impact velocity and impact angle corresponding to the two sets of simulations are compared in Figure 7. The correlation is accounted for using the linear correlation coefficient of -0.48, as obtained from the rockfall simulations. The difference observed between the two sets of couples $(V_{r,i}, \alpha_{r,j})$ results from consideration of this correlation through the Gaussian standardization method, presented in appendix.

4 Probabilistic analysis of the fence efficiency

4.1 Influence of the velocity

Impact simulations for the 5 different values of the velocity V_r presented in Table 4 and for an impact angle set at $\alpha_r = 34.8^{\circ}$, corresponding to the mean impact angle in the rockfall simulations, are first analyzed. The values of the

Table 4 Results of selected rockfall simulations for 5 different values of the velocity V_r and for an impact angle set at $\alpha_r = 34.8^\circ$.

V_r (m/s)	3.10	4.47	6.23	8.69	12.55
G (-)	-0.495	-0.516	-0.438	-0.258	0.529

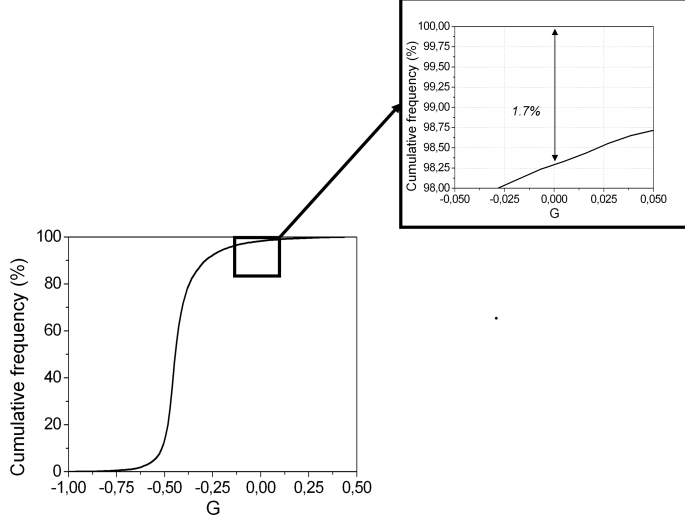


Fig. 8 Cumulative distribution of the performance function $G = \frac{V_{z,out}}{V_{z,in}}$ under loading conditions for which V_r is the only random variable.

performance function G obtained for these simulations are exposed in Table 4. The fence does not fulfill its protection function and the block is not stopped when the velocity is 12.55 m/s ($G > 0$).

The cumulative distribution of the performance function G considering only V_r as a random variable is given in Figure 8. It clearly shows that the probability for having $G > 0$ is 1.7%. Assuming that the event $G > 0$ can be associated with the larger impact velocity values, it can be deduced that the 1.7% of the loading cases leading to a fence clearing correspond to the 1.7% larger velocities.

Consequently, the maximum admissible velocity by the fence is deduced from the cumulative distribution of the lognormal distribution of V_r (Fig. 9) corresponding to the rockfall simulation results (Fig. 5). This value is approximately $V_{r,max} = 9.7 \text{ m/s}$ (Fig. 9). The corresponding maximum translational impact energy is $E_{c,max} = 1/2 m_{rock} V_{r,max}^2 = 22.5 \text{ kJ}$.

4.2 Influence of the two variables, considered as non correlated

The results from the first simulations set were analyzed considering the impact velocity as a random variable and the impact angle as a deterministic

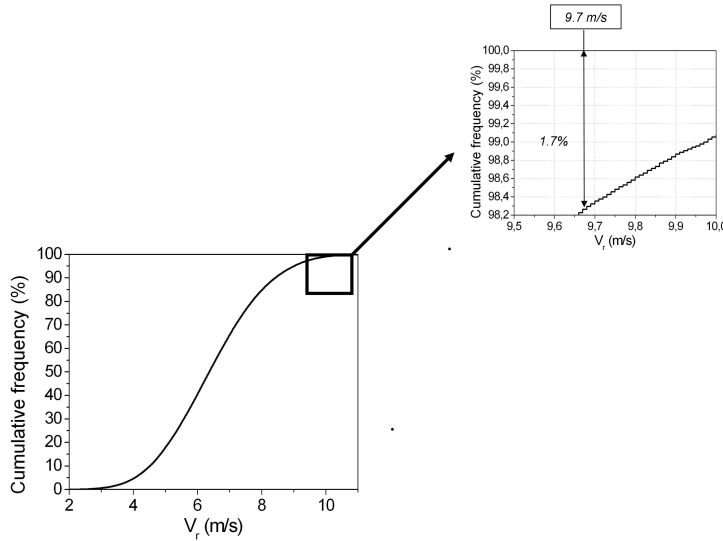


Fig. 9 Cumulative distribution of V_r .

parameter but for different impact angles. This analysis allowed determining the cumulative distribution of the performance function G for different impact angles. This cumulative distribution is strongly influenced by the impact angle (Fig. 10). The most critical cases, leading to larger probabilities for positive values of G , result from impacts oriented downwards and with shallow incidence with respect to the wire mesh plane.

For each value of the impact angle considered, the probability for having $G > 0$ was measured using the cumulative distribution of G . The maximum admissible impact velocity and the corresponding translational impact energy were deduced from this probability following the same principle as exposed previously for an impact angle set at $\alpha_r = 34.8^\circ$ (Figs. 8 and 9). The maximum admissible impact energy was shown to be significantly depending on the impact angle considered (Fig. 11). In particular, the maximum admissible energy drastically decreases for shallow impacts.

4.3 Influence of the two variables, considering the correlation

The second set of 25 simulations allowed characterizing the cumulative distribution of G considering the linear correlation existing between the two variables.

The fence failure probability in such a case is calculated from the cumulative distributions of G (Fig. 12). The comparison with the case where variables are considered non correlated, plotted on the same figure, shows that integrating the correlation is slightly conservative as the probability for the block

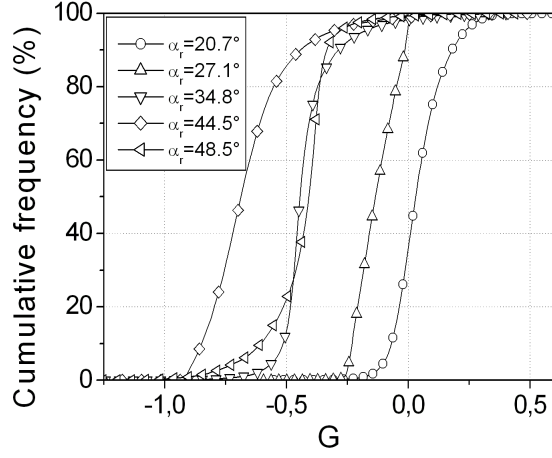


Fig. 10 Cumulative distribution of the performance function G under loading conditions for which V_r is the only random variable and for different impact angles α_r .

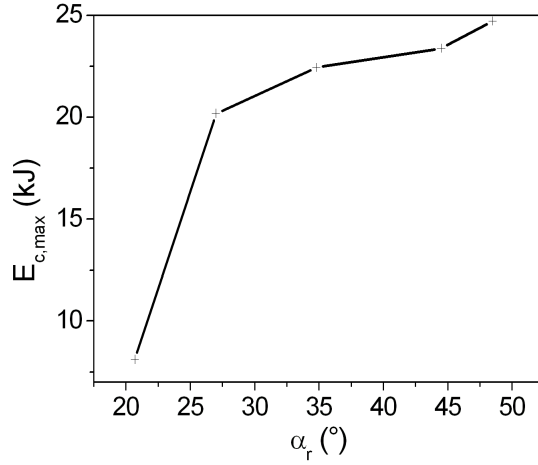


Fig. 11 Maximum energy $E_{c,max}$ without fence clearing for different impact angles α_r .

to clear the fence is larger when correlated variables are considered. Without correlation, this probability is 4.2% whereas it is 7.6% considering the correlation.

More notably, the comparison with Figure 8 shows that considering the only velocity as a random variable leads to optimistic results with a clearing probability of 1.7% only.

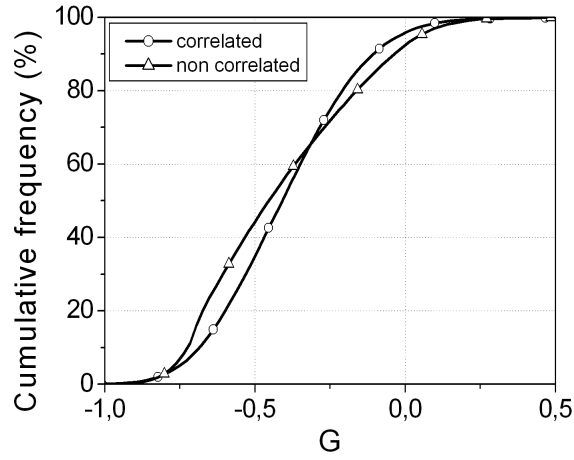


Fig. 12 Cumulative distribution of the performance function G under loading conditions for which V_r and α_r are the only random variables.

5 Conclusion

In this paper, an approach aiming at improving the design of rockfall protection fences has been proposed. The design facet concerned here is the ability of the fence to stop the block, provided the fence height has been well determined. Traditionnally, theses structures are designed considering the energy of the block to be intercepted disregarding other parameters associated to the block kinematics, mainly because it is computation-time demanding. On the contrary, the approach proposed aims at reducing the number of simulations to be performed while providing statistically relevant data with respect to the fence efficiency, thus making more exhaustive studies affordable.

This approach couples blocks propagation simulations with numerical simulations of the fence impacted by the block. The use of trajectory simulation results ensures that the site specific loadings are considered for the design of the fence. In addition, as the loading parameters are considered as random variables, the variability of the loading conditions in the site is also introduced in the calculation for the fence design.

The feasibility of the approach was appraised on a specific study case. The probability for the clearing of a protection fence was examined considering a variable loading of the fence related with two random variables : the impact velocity and the impact angle of the rock. The fence failure probability was assessed considering successively one random variable (velocity), then the two variables either considered non correlated or linearly correlated.

The results obtained for the case study first show that the approach can be applied to calculate the probability for the fence failure. The interest for the

designer also appears clearly. Classically, conducting a statistically relevant analysis considering two variables would require several hundreds of impact simulations while only 25 are necessary with this approach.

Conclusions concerning the response of the fence and its sensitivity to the variable considered can also be drawn. In the case of only one random variable, a maximum allowable impact energy was determined from the fence failure probability. However, this maximum impact energy is strongly depending on the values of the deterministic loading parameters (incidence angle in particular). This quantity is thus not an absolute indicator of the fence capacity that can be generalized to different loading conditions, that is on another site.

The number of random variables strongly influences the probability for the fence clearing. If one random variable is considered, the probability for the fence clearing is strongly depending on the values of the deterministic loading parameters. The impact angle has been shown to have a significant influence on the fence failure probability, with a ratio of more than two over the impact angle range considered. This parameter should be considered when designing fences, together with the block mass and velocity.

This approach appears promising in terms of fence design improvement for it allows investigating the influence of many variables. It also allows improving the quantification of the residual hazard in the site after installing the structure. Nevertheless, the influence of other parameters should be investigated, as for instance the impact point location on the fence, and the orientation of the block with respect to the fence perpendicular axis.

Acknowledgements This research was completed within the framework of the research network Natural Hazards and Vulnerability of Structures (VOR). This network is funded by the French Ministry of Research and combines different laboratories in the Rhône-Alpes region.

References

1. Baroth J, Schoefs F, Breyse D (2012) Construction reliability. Wiley, London.
2. Baroth J, Bressolette P, Chauvire C, Fogli M (2007) An efficient SFE method using Lagrange polynomials: application to nonlinear mechanical problems with uncertain parameters. *Comp Meth Appl Mech Eng* 196: 4419-4429.
3. Bertrand D, Nicot F, Gotteland P, Lambert S (2008) DEM numerical modeling of double-twisted hexagonal wire mesh. *Can Geotech J* 45: 1104-1117.
4. Bertrand D, Trad A, Limam A, Silvani C (2012) Full-scale dynamic analysis of an innovative rockfall fence under impact by the discrete element method. From the local scale to the structure scale. *Rock Mech Rock Eng* 45(5): 885-900.
5. Bourrier F, Dorren LKA, Nicot F, Berger F, Darve F (2009) Toward objective rockfall trajectory simulation using a stochastic impact model. *Geomorphology* 110: 6879.
6. Bourrier F, Bigot C, Bertrand D, Lambert S, Berger F (2010) A numerical model for the design of low energy rockfall protection nets. In: proceedings of the Third Euro-Mediterranean Symposium on Advances in Geomaterials and Structures, Djerba, Tunisia.
7. Buzzi O, Spadari M, Giacomini A, Fityus S, Sloan SW (2012) Experimental testing of rockfall barriers designed for the low range of impact energy. *Rock Mech Rock Eng*. doi: 10.1007/s00603-012-0295-1.
8. Cazzani HG, Mongioli L, Frenet T (2002) Dynamic finite element analysis of interceptive devices for falling rocks. *Int J Rock Mech Min* 39: 303-321.

9. Cundall PA, Strack ODL (1979) A discrete numerical model for granular assemblies. *Geotechnique* 29 (1): 47-65.
10. Dorren LKA, Berger F, Putters US (2006) Real size experiments and 3D simulation of rockfall on forested and non-forested slopes. *Nat Hazard Earth Sys* 6:145-153.
11. EOTA (2008) Guidelines for European technical approval of falling rock protection kits (ETAG 027). February 2008, Brussels.
12. Gerber W, Boell A (2006) Type-testing of rockfall barriers -comparative results Int: *Proceedings of the Interpraevent Congress*, Nigata, Japan.
13. Gentilini C, Govoni L, Miranda S, Gottardi G, Ubertini F (2012) Three-dimensional numerical modelling of falling rock protection barriers. *Comput Geotech* 44: 58-72.
14. Gottardi G, Govoni L (2010) Full-scale modelling of falling rock protection barriers. *Rock Mech Rock Eng* 43(3): 261-274.
15. Grassl H, Volkwein A, Anderheggen E, Ammann WJ (2002) Steel-net rockfall protection - experimental and numerical simulations. In: *Proceedings of the Seventh international conference on structures under shock and impact*, Montreal, Canada.
16. Hearn G, Barrett RK, Henson HH (1996) Testing and modelling of two rockfall barriers. *Transp Res record* 1504: 1-11.
17. Lambert S, Bertrand D, Berger F, Bigot C (2010) Low energy rockfall protection fences in forested areas: Experiments and numerical modeling. In: *Prediction and Simulation Methods for Geohazard Mitigation*, Kyoto, Japan.
18. Lambert S, Bourrier F (2013) Design of rockfall protection embankments: a review. *Eng Geol* 154: 77-88.
19. Nicot F, Cambou B, Mazzoleni G (2001) Design of rockfall restraining nets from a discrete element modelling. *Rock Mech Rock Eng* 34: 98118.
20. Peila D, Pelizza S, Sassudelli F (1998) Evaluation of Behaviour of rockfall restraining nets by full scale tests. *Rock Mech Rock Eng* 21(1): 1-24.
21. Smilauer V, Catalano E, Chareyre B, Dorofeenko S, Duriez J, Gladky A, Kozicki J, Modenese C, Scholtes L, Sibille L, Strnsky J, Thoeni K (2010) *Yade Documentation* (V. Smilauer, ed.), The Yade Project, 1st ed. <http://yade-dem.org/doc/>.
22. Stokes A, Salin F, Kokutse AD, Berthier S, Jeannin H, Mochan S, Dorren LKA, Kokutse N, Abd-Ghani M, Fourcaud T (2005) Mechanical resistance of different tree species to rockfall in the French Alps. *Plant Soil* 278(1-2): 107-117.
23. Thoeni K, Lambert C, Giacomini A, Sloan SW (2013) Discrete modelling of hexagonal wire meshes with a stochastically distorted contact model. *Comput Geotech* 49: 158-169.
24. Van Tran P, Maegawa K, Fukada S (2012) Experiments and Dynamic Finite Element Analysis of a Wire-Rope Rockfall Protective Fence. *Rock Mech Rock Eng*. doi 10.1007/s00603-012-0340-0
25. Volkwein A, Roth A, Gerber W, Vogel A (2009) Flexible rockfall barriers subjected to extreme loads. *Structural engineering international* 19: 327 332.

A Gaussian standardization of two correlated log-normal random variables

Let $\mathbf{Y} = (Y_1, Y_2)$ be a 2D lognormal random variable with given mean $\mu_Y = (\mu_{Y_1}, \mu_{Y_2})$ and standard deviation $\sigma_Y = (\sigma_{Y_1}, \sigma_{Y_2})$ and coefficient of correlation $\rho_{Y_1 Y_2}$. In this case, the Gaussian standardization of \mathbf{Y} writes:

$$\mathbf{Y} = T(\mathbf{X}) \Leftrightarrow \begin{cases} Y_1 = \frac{\mu_{Y_1}}{\sqrt{1+Cv_{Y_1}^2}} \exp\{L_{11}X_1\} \\ Y_2 = \frac{\mu_{Y_2}}{\sqrt{1+Cv_{Y_2}^2}} \exp\{L_{21}X_1 + L_{22}X_2\} \end{cases} \quad (4)$$

with:

$$L_{11} = \sqrt{\ln(1 + Cv_{Y_1}^2)} \quad (5)$$

$$L_{21} = \frac{\ln(1 + \rho_{Y_1 Y_2} Cv_{Y_1} Cv_{Y_2})}{L_{11}} \quad (6)$$

$$L_{22} = \sqrt{\frac{\ln(1 + Cv_{Y_1}^2) \ln(1 + Cv_{Y_2}^2) - \ln^2(1 + \rho_{Y_1 Y_2} Cv_{Y_1} Cv_{Y_2})}{L_{11}^2}} \quad (7)$$

where $Cv_{Y_i} = \frac{\sigma_{Y_i}}{\mu_{Y_i}}$, $i = 1, 2$ are the coefficients of variation of Y_1 and Y_2 .